

Solvent-Induced Modulation of Collective Photophysical Processes in Fluorescent Silica Nanoparticles

Marco Montalti,* Luca Prodi, Nelsi Zaccheroni, and Giuseppe Falini

Contribution from the Dipartimento di Chimica "G. Ciamician",
Via Selmi 2, 40126 Bologna, Italy

Received June 12, 2002

Abstract: In this paper we show how it is possible to control the nature and the efficiency of collective photophysical processes in a network composed of two different fluorescent units organized on the surface of silica nanoparticles. Such a structure is obtained by covering nanoparticles with a layer of dansyl moieties (Dns) and by partially protonating them in solution. The two fluorophores Dns and Dns·H⁺ have very different photophysical properties and can be selectively excited and detected. The interaction between the two units Dns and Dns·H⁺ has been first investigated in a reference compound obtained by derivatizing 1,6-hexanediamine with two dansyl units. The photophysical characterization of this compound (absorption spectra, fluorescence spectra, quantum yield, and lifetime) showed that the two moieties can be involved both in energy and electron-transfer processes. Dansylated nanoparticles were prepared by modifying preformed silica nanoparticles with dansylated (3-aminopropyl)trimethoxysilane. Photophysical studies indicated that protonation has a dramatic effect on the fluorescence of the nanoparticles, leading to the quenching of both the protonated units and the surrounding nonprotonated ones. This amplified response to protonation, due to charge-transfer interactions, is solvent-dependent and is less efficient in pure chloroform with respect to acetonitrile/chloroform (5/1 v/v) mixtures. The reduced efficiency of the electron-transfer processes responsible for the quenching makes energy transfer competitive to such an extent that in pure chloroform excitation energy migration takes place from Dns·H⁺ to Dns with great efficiency.

Introduction

The organization of photophysically active units in broad structures typically gives rise to collective effects that can be exploited for the design of new functional materials.¹ Different strategies were followed to achieve organized multichromophoric systems leading to the development of photoactive polymers,¹ dendrimers,² zeolites,³ and self-assembled monolayers.⁴

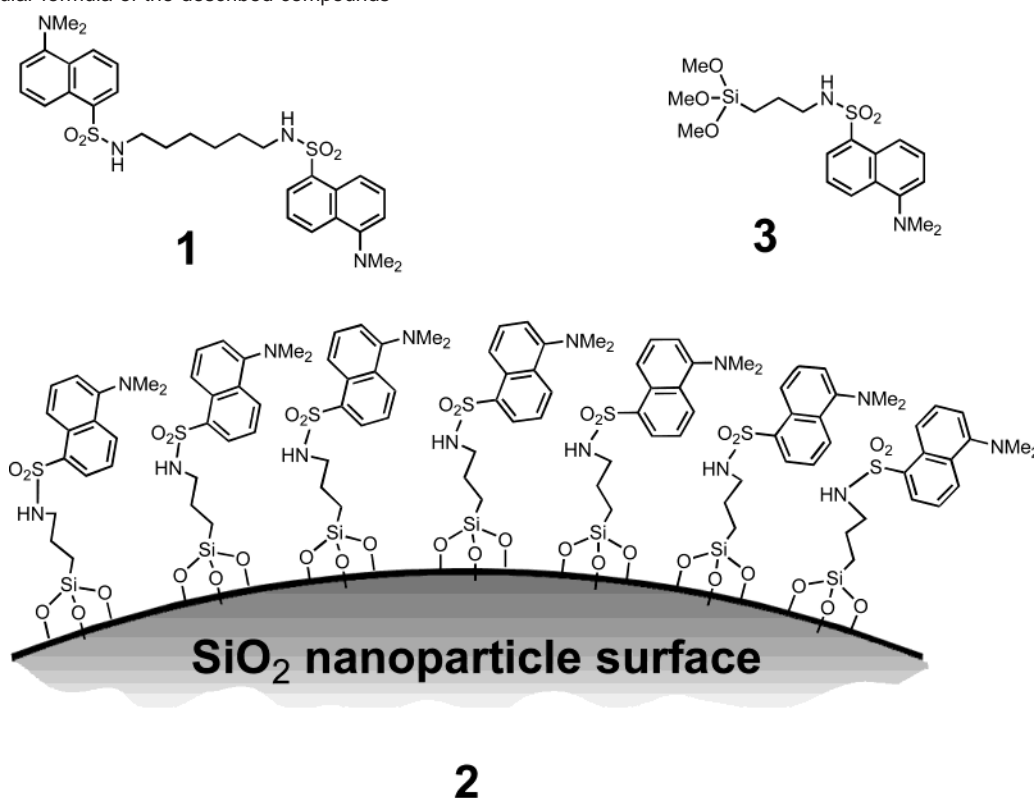
Modification of the surface of nanoparticles is a suitable and still almost unexplored path to constrain a set of fluorescent units into an organized network. Fluorescent nanoparticles are in fact very promising for the design of labels and sensors for the relative ease of their synthesis and for their peculiar properties. Even if some examples of dye adsorption have been reported as a possible approach to nanoparticle surface modification,⁵ covalent grafting⁶ is necessary to obtain a stable arrangement and avoid structural reorganizations due to redistribution of the dye on the surface or between the surface and the solution. Silica nanoparticles can be prepared in a very straightforward way and their surface can be easily modified by means of alcoxysilane derivatives. This versatility makes,

in our opinion, silica nanoparticles a good choice as a scaffolding structure for a network of dye moieties, especially considering that in addition these materials are transparent to visible light and inert as far as energy and electron-transfer processes are concerned.^{5d} As a consequence, dye-coated silica nanoparticles constitute a suitable system to characterize intermolecular

* Address correspondence to this author: e-mail mmont@ciam.unibo.it.

(1) (a) Swager, M. T. *Acc. Chem. Res.* **1998**, *31*, 201. (b) McQuade, D. T.; Pullen, A. E.; Swager, T. M. *Chem. Rev.* **2000**, *100*, 2537. (c) Kim, J.; McQuade, D. T.; Rose, A.; Zhu, Z.; Swager, T. M. *J. Am. Chem. Soc.* **2001**, *123*, 11488. (d) McQuade, D. T.; Hegedus, A. H.; Swager, T. M. *J. Am. Chem. Soc.* **2000**, *122*, 12389. (e) Levitsky, I. A.; Kim, J.; Swager, T. M.; *Macromolecules* **2001**, *34*, 2315. (f) Fleming, C. N.; Maxwell, K. A.; De Simone, J. M.; Meyer, T. J.; Papanikolas, J. M. *J. Am. Chem. Soc.* **2001**, *123*, 10336.

(2) (a) Vögtle, F.; Gestermann, S.; Kauffmann, C.; Ceroni, P.; Vicinelli, V.; De Cola, L.; Balzani, V. *J. Am. Chem. Soc.* **1999**, *121*, 12161. (b) Vögtle, F.; Gestermann, S.; Kauffmann, C.; Ceroni, P.; Vicinelli, V.; Balzani, V. *J. Am. Chem. Soc.* **2000**, *122*, 10398. (c) Venturi, M.; Serroni, S.; Juris, A.; Campagna, S.; Balzani, V. *Top. Curr. Chem.* **1998**, *197*, 193. (d) Balzani, V.; Campagna, S.; Denti, G.; Juris, A.; Serroni, S.; Venturi, M. *Acc. Chem. Res.* **1998**, *31*, 26. (e) Archut, A.; Vögtle, F.; De Cola, L.; Azzellini, G. C.; Balzani, V.; Ramanujam, P. S.; Berg, R. H. *Chem. Eur. J.* **1998**, *4*, 699. (f) Archut, A.; Azzellini, G. C.; Balzani, V.; De Cola, L.; Vögtle, F. *J. Am. Chem. Soc.* **1998**, *120*, 12187. (g) Vicinelli, V.; Ceroni, P.; Maestri, M.; Balzani, V.; Gorka, M.; Vögtle, F. *J. Am. Chem. Soc.* **2002**, *124*, 6461. (h) Balzani, V.; Ceroni, P.; Gestermann, S.; Gorka, M.; Kauffmann, C.; Vögtle, F. *J. Chem. Soc., Dalton Trans.* **2000**, 3765. (3) (a) Pauchard, M.; Huber, S.; Méallet-Renault, R.; Maas, H.; Pansu, R.; Calzaferri, G. *Angew. Chem., Int. Ed.* **2001**, *40*, 2839. (b) Pauchard, M.; Devaux, A.; Calzaferri, G. *Chem. Eur. J.* **2000**, *6*, 3456. (4) (a) Flink, S.; van Veggel, F. C. J. M.; Reinhoudt, D. N. *Chem. Commun.* **1999**, 2229. (b) Christoffels, L. A. J.; Andronov, A.; Fréchet, J. M. J. *Angew. Chem., Int. Ed.* **2000**, *39*, 2163. (c) van der Veen, N. J.; Menno, S. F.; Deij, A.; Egberink, R. J. M.; van Veggel, F. C. J. M.; Reinhoudt, D. N. *J. Am. Chem. Soc.* **2000**, *122*, 6112. (5) (a) Shipway, A. N.; Lavah, M.; Gabai, R.; Willner, I. *Langmuir* **2000**, *16*, 8789. (b) Nakashima, K.; Yasuda, S.; Nishihara, A.; Yamashita, Y. *Colloids Surf.* **1998**, *139*, 251. (c) Nasr, C.; Liu, D.; Hotchandani, S.; Kamat, P. V. *J. Phys. Chem.* **1996**, *100*, 11054. (d) Heimer, T. A.; Meyer, G. J. *J. Lumin.* **1996**, *70*, 468. (e) Farzad, F.; Thompson, D. W.; Kelly, C. A.; Meyer, G. J. *J. Am. Chem. Soc.* **1999**, *121*, 5577. (f) Caruso, F.; Donath, E.; Möhwald, H. *J. Phys. Chem.* **1998**, *102*, 2011. (g) Caruso, F.; Donath, E.; Möhwald, H.; Georgieva, R. *Macromolecules* **1998**, *31*, 7365. (6) Beck, C.; Härtl, W.; Hempelmann, R. *Angew. Chem., Int. Ed.* **1999**, *38*, 1297.

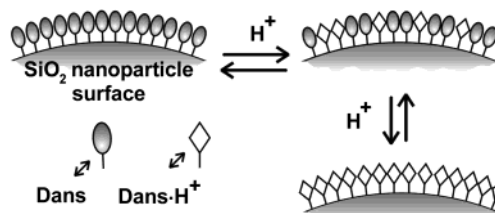
Chart 1. Molecular formula of the described compounds

photophysical processes at their surface, avoiding any interference from the particle nucleus.

Among the different dyes, we choose the dansyl group [5-(dimethylamino)-1-naphthalenesulfonamido], Dns, because of the peculiar response of its photophysical properties to the protonation of the amino group. The lowest excited state of dansyl has, in fact, a charge-transfer character involving the promotion of a lone-pair electron of the amino group into a π antibonding orbital of the naphthalene ring.⁷ In the $\text{Dns}\cdot\text{H}^+$ unit this charge transfer state is destabilized and the $\pi-\pi^*$ transition localized on the naphthalene becomes the lowest in energy. This leads to a strong blue shift of both the absorption and luminescence bands that allows us, in partially protonated polydansylated systems, to selectively excite and detect the outcoming fluorescence of the two different units. Hence, a polydansylated system represents a good example of a network composed by two different kinds of chromophores (Dns and $\text{Dns}\cdot\text{H}^+$) whose relative composition can be controlled by changing the degree of protonation (Scheme 1).^{2a}

The fluorescent nanoparticles **2** described in the present work bear an average number of about 4000 dansyl units each and were prepared by covering preformed silica colloids with the silane derivative (Chart 1). The main goal of the photophysical investigation was to analyze the cooperative effects that arise from the organization of several chromophoric units into a high-density pattern as found at the surface of these nanoparticles.

This investigation requires, of course, information about the nature of the interaction between the two chromophores (Dns

Scheme 1. Schematic Representation of the Behavior of Dansylated Nanoparticles as a Two-Fluorophore Network Whose Composition Is Controlled through Protonation

and $\text{Dns}\cdot\text{H}^+$) forming the network. For this purpose, we synthesized the bisdansylated reference compound **1** and we explored the effects of protonation on its photophysical properties, finding that both energy and electron-transfer processes can occur between the two units Dns and $\text{Dns}\cdot\text{H}^+$. It was interesting to see that the same photophysical processes occurring in the dimer **1** could be also observed in the nanoparticles **2**. In the latter case, however, they are no longer localized on a single pair of units, leading to very different behavior between systems **1** and **2** that can be clearly attributed to the occurrence, in the organized network, of photophysical processes involving multicomponent interactions. As a consequence, the chemical input represented by a local modification (protonation of one Dns unit) affects the properties of the surrounding unmodified units, which respond to the confined input with a change in their fluorescence. This means that the signal modulation involves a number of units much larger than those effectively affected by the chemical modification, so that the chemical input is translated in an amplified fluorescence response.

We also observed that for nanoparticles **2** the fluorescence output is strongly dependent on solvent polarity and the behavior

(7) (a) Prodi, L.; Bolletta, F.; Montalti, M.; Zaccheroni, N. *Eur. J. Inorg. Chem.* **1999**, 5, 445. (b) Corradini, R.; Dossena, A.; Marchelli, R.; Panaria, A.; Sartor, G.; Saviano, M.; Lombardi, A.; Pavone, V. *Chem. Eur. J.* **1996**, 2, 373. (c) Ikeda, H.; Nakamura, M.; Ise, N.; Oguma, N.; Nakamura, A.; Ikeda, T.; Toda, F.; Ueno, A. *J. Am. Chem. Soc.* **1996**, 118, 980. (d) Prodi, L.; Montalti, M.; Zaccheroni, N.; Dallavalle, F.; Folesani, G.; Lanfranchi, M.; Corradini, R.; Pagliari, S.; Marchelli, R. *Helv. Chim. Acta* **2001**, 84, 690.

Table 1. UV-vis Absorption Data for **1** and **2** in the Neutral and Protonated Forms

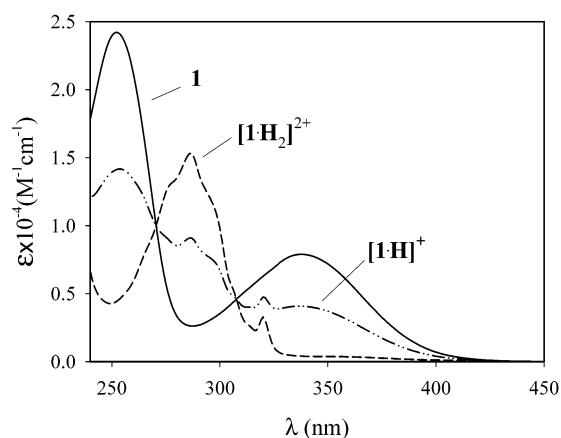
	absorbance			
	CH ₃ CN/CHCl ₃ (5/1 v/v)		CHCl ₃	
	λ_{\max} (nm)	ϵ (M ⁻¹ cm ⁻¹)	λ_{\max} (nm)	ϵ (M ⁻¹ cm ⁻¹)
1	338	7900	339	7800
	253	24 500	254	24 900
[1 ·H ₂) ²⁺ ^a	286	15 000	288	14 500
2	338		337	
	252		253	
protonated 2 ^a	287		289	

^a After addition of an excess of CF₃SO₃H.

Table 2. Fluorescence Data for **1** and **2** in the Neutral and Protonated Forms

	fluorescence			
	CH ₃ CN/CHCl ₃ (5/1 v/v)		CHCl ₃	
	λ_{\max}	Φ (τ /ns)	λ_{\max}	Φ (τ /ns)
1	510	0.25 (13)	500	0.28 (13)
[1 ·H] ⁺ ^a	510	0.03 (1.8) ^b	500	0.10 (3.7) ^b
	336	<0.01 ^d	336	<0.01 ^d
[1 ·H ₂) ²⁺ ^c	336	0.03 ^d	336	0.03 ^d
2	514	0.26 (13)	512	0.28 (13)
protonated 2 ^c	336	0.03	336	0.03

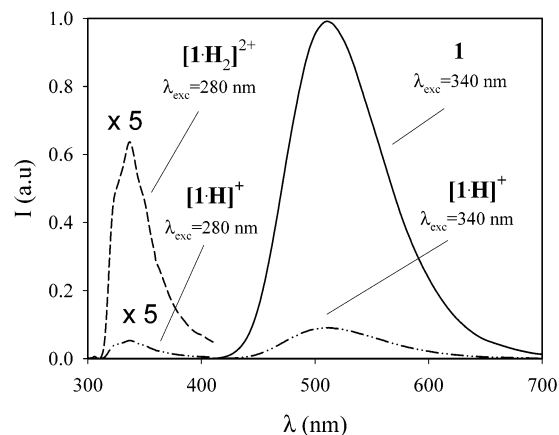
^a Calculated with SPECFIT software. ^b After protonation of 90% of the Dns units. ^c After addition of an excess of CF₃SO₃H. ^d τ < 1.0 ns.

**Figure 1.** Absorption spectra of the reference compound **1** and its protonated forms in CH₃CN/CHCl₃ (5/1 v/v). [**1**·H₂)²⁺ spectrum resulted from fitting of the spectra recorded during the titration with CF₃SO₃H by the global analysis SPECFIT program.⁹

of the system can be modulated by changing the environmental conditions. This tunability makes these systems extremely promising for the design of new fluorescence-based sensors.^{1a}

Results and Discussion

Protonation of Reference Compound 1. The reference compound **1** shows the typical absorption and fluorescence bands of dansyl derivatives (Tables 1 and 2 and Figures 1 and 2).⁷ Both the lowest energy absorption band and the fluorescence band are associated with a transition involving an excited state having a considerable charge-transfer character due to the promotion of a lone-pair electron of the amino group into a π antibonding orbital of the naphthalene ring. Because of its nature, the energy of this excited state is very sensitive to the polarity of the solvent,⁷ as demonstrated by the 10 nm shift of the fluorescence maximum observed on going from pure chloroform to the chloroform/acetonitrile mixture.

**Figure 2.** Fluorescence spectra of the reference compound **1** and of its protonated forms in CH₃CN/CHCl₃ (5/1 v/v). [**1**·H₂)²⁺ spectra resulted from fitting of the spectra recorded during the titration with CF₃SO₃H by the global analysis SPECFIT program.⁹

Protonation experiments on compound **1** were carried out both in pure chloroform and in acetonitrile/chloroform (5/1 v/v) by adding to an 8.1×10^{-6} M solution of the dimer increasing amounts of solutions of CF₃SO₃H ($c = 10^{-4}$ and 10^{-3} M).

Protonation of the amino group causes a gradual disappearance of the charge-transfer band in the absorption spectrum and the concomitant appearance of a new band that has the typical structure and energy of naphthalene derivatives (Figure 1). Two isosbestic points are maintained during the titration in both solvents. Upon excitation at $\lambda_{\text{exc}} = 280$ nm, where Dns·H⁺ absorbs most of the light, a new fluorescence band at 336 nm can be detected. The photophysical properties of compound **1** in the presence of an excess of triflic acid are reported in Tables 1 and 2 and Figures 1 and 2. The dramatic changes of the photophysical properties of the dansyl unit upon protonation have been previously attributed to the modification of the nature of the lowest energy excited state that, losing its charge-transfer character, becomes a pure π - π^* transition localized on the naphthalene ring.⁷

The two luminescence signals at 340 and 510 nm, upon excitation at 280 and 340 nm, respectively, are reported in Figure 3. The observed changes are represented as a function of the fraction of protonated Dns units in the solution instead of just referring them to the amount of acid added, which is not a good indicator of the composition of the system since protonation is not always quantitative.

This parameter can be obtained in a very direct way. Absorption data, in fact, indicate that the spectra of all the species in solution are simply the sum of the spectra of the units by which they are composed and that mutual interaction in the ground state can be ruled out. As a consequence, the fraction of Dns·H⁺ units can be directly calculated from absorbance.⁸ Two major features of diagrams reported in Figure 3 can be noted. The first one is that, at the beginning of the titration, when only a small fraction of acid is added leading mostly to the formation of the **1**·H⁺ species, the protonation of a single moiety causes a decrease in the luminescence intensity comparable with the quenching of two dansyl units. The second feature to note is that under these conditions the disappearance

(8) The fraction of Dns·H⁺ was calculated from the absorption at 280 nm as $(A - A_i)/(A_f - A_i)$ where A , A_i , and A_f are respectively the absorbance during, at the beginning, and at the end of the titration with CF₃SO₃H.

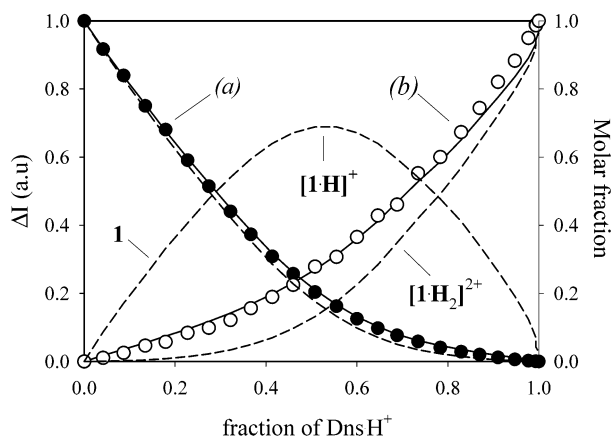


Figure 3. Normalized luminescence intensity changes of a solution of **1** [8×10^{-6} M in $\text{CH}_3\text{CN}/\text{CHCl}_3$ (5/1 v/v)] as a function of the degree of protonation calculated from the absorbance at 280 nm: (a) $\lambda_{\text{exc}} = 340$ nm, $\lambda_{\text{em}} = 510$ nm; (b) $\lambda_{\text{exc}} = 280$ nm, $\lambda_{\text{em}} = 340$ nm.⁸ The dashed lines represent the molar fractions of the different species as resulting from the fitting with SPECFIT; solid lines describe the related fitted luminescence intensity.⁹

of the dansyl luminescence does not correspond to an equivalent increase of the luminescence typical of $\text{Dns}\cdot\text{H}^+$. These two findings suggest that protonation of a single dansyl unit in **1** leads to the substantial quenching of the luminescence of both Dns and $\text{Dns}\cdot\text{H}^+$. Interpolation of absorption and fluorescence titration profiles with the global analysis package SPECFIT⁹ confirmed this qualitative interpretation, allowing us to calculate the fluorescence spectra of $1\cdot\text{H}^+$ (Table 2 and Figure 2), the molar fraction distribution of all the species in solution (Figure 3), and the constants relative to the two protonation steps [$\log K_1 = 8.5 \pm 0.5$ and $\log K_2 = 7.2 \pm 0.5$ in acetonitrile/chloroform (5/1 v/v), and $\log K_1 = 6.3 \pm 0.1$ and $\log K_2 = 5.2 \pm 0.1$ in pure chloroform]. To better understand the behavior of **1** upon protonation, we measured the excited-state lifetime of the residual fluorescence of the Dns unit ($\lambda_{\text{exc}} = 340$ nm, $\lambda_{\text{em}} > 450$ nm) of solutions of **1** after the protonation of 90% of the dansyl units.

Under these conditions, $1\cdot\text{H}^+$ is by far prevalent with respect to **1**, while $1\cdot\text{H}_2^{2+}$ does not interfere since it is not luminescent in the spectral region under investigation. As it can be seen in Table 2, the decrease of the luminescence quantum yield of Dns observed on going from **1** to $1\cdot\text{H}^+$ is parallel, in both the solvents examined, with the shortening of the excited-state lifetime. Similar protonation experiment carried out on dansylated dendrimers have been interpreted on the basis of energy-transfer processes involving the Dns and $\text{Dns}\cdot\text{H}^+$ moieties.^{2a} As can be seen from Figure 4, however, the quenching of the fluorescent excited state of Dns units cannot be attributed to such processes since this same state is the lowest in energy of the whole system. In addition, it is noted that the efficiency of the quenching of the Dns moiety in $1\cdot\text{H}^+$ depends on the solvent polarity (Table 2).

This finding suggests that the observed quenching could be due to an electron-transfer process from Dns to $\text{Dns}\cdot\text{H}^+$. To support this conclusion, we have performed electrochemical experiments in acetonitrile solutions, showing that dansylamide undergoes a chemically irreversible oxidation process with E_p

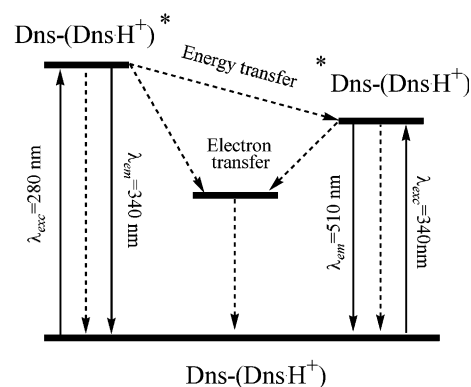


Figure 4. Simplified diagram of the electronic states for the species $[1\cdot\text{H}]^+$.

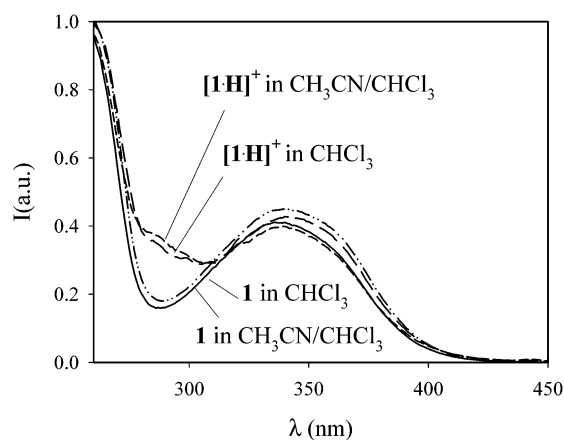


Figure 5. Excitation spectra of solutions of **1** ($c = 8 \times 10^{-6}$ M) in CHCl_3 and $\text{CH}_3\text{CN}/\text{CHCl}_3$ (5/1 v/v); $\lambda_{\text{em}} = 510$ nm. Excitation spectra of $[1\cdot\text{H}]^+$ are relative to the same **1** solutions after protonation of 90% Dns units.⁸

$= 0.91$ V vs standard calomel electrode (SCE), in agreement with what was previously reported for a similar dansyl derivative,^{2g,h} while its protonated form undergoes an irreversible reduction process with $E_p = -1.37$ V vs SCE. The energy of the fluorescent excited state of the Dns unit, 2.75 eV as estimated from the onset of its fluorescence band,^{2g,h} is then largely sufficient to make the electron transfer process thermodynamically allowed ($\Delta G \approx -0.4$ eV).

On the contrary, when the $\text{Dns}\cdot\text{H}^+$ unit is excited, both energy and electron-transfer processes are thermodynamically allowed. The estimated energy of the fluorescent excited state of $\text{Dns}\cdot\text{H}^+$ (3.8 eV) is in fact ca. 1 eV higher than that of the Dns chromophore. In the excitation spectra taken after protonation of 90% of the dansyl units and recorded at $\lambda_{\text{em}} = 510$ nm, i.e., looking at the emission of the Dns unit, the presence of a contribution of a band in the spectral region where $\text{Dns}\cdot\text{H}^+$ absorbs can be clearly detected (Figure 5). This finding unambiguously reveals the occurrence of an energy-transfer process from the $\text{Dns}\cdot\text{H}^+$ excited state to the Dns moiety. However, the efficiency of such a process is far from being unitary. The contribution of the band of $\text{Dns}\cdot\text{H}^+$ in the excitation spectra is, in fact, much lower than its contribution in the absorption spectra, indicating that only a limited fraction of excitation energy is transferred from $\text{Dns}\cdot\text{H}^+$ to the Dns localized excited state. As a consequence, this deactivation process alone is not sufficient to explain the large quenching observed for the $\text{Dns}\cdot\text{H}^+$ moieties, and also in this case electron transfer seems to be not only likely but even the most efficient process.

(9) (a) Binstead, R. A. *SPECFIT*; Spectrum Software Associates: Chapel Hill, NC, 1996. (b) Gampp, H.; Maeder, M.; Meyer, C. J.; Zuberbühler, A. D. *Talanta* **1985**, *32*, 257.

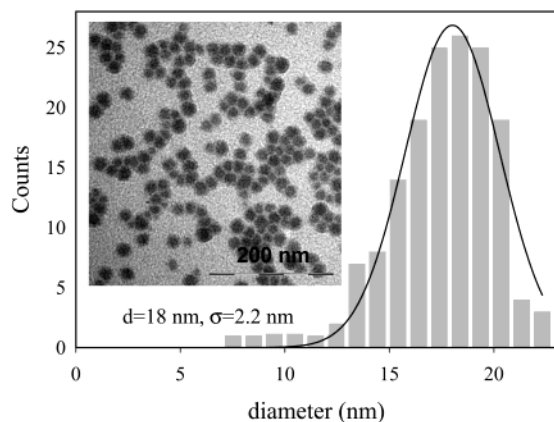


Figure 6. Size distribution of the dansylated nanoparticles **2** calculated from TEM images (see for example the inset picture). The solid line represents the Gaussian fitting of the distribution.¹⁰

Characteristics of Dansylated Nanoparticles 2. Graphical elaboration of TEM images of nanoparticles **2** (see for example Figure 6) allowed the determination of the average diameter and the dispersion ($d = 18.0$ nm with $\sigma = 2.2$ nm) of the nanoparticles.¹⁰ The degree of surface coverage could be calculated from the dansyl absorbance⁷ of solutions containing a known amount of nanoparticles, assuming them to be spherical and making reference to the surface area declared by Aldrich. The average number of about 4000 dansyl units per nanoparticle obtained is compatible with a density of one moiety every 25 Å², in agreement with what reported for grafting of silica surfaces with unmodified (3-aminopropyl)trimethoxysilane.^{4a} The closeness of the dansyl moieties was confirmed by measurements of fluorescence polarization in PVC films by comparing nanoparticles **2** with dansylamide. In the polymeric matrix, rotational relaxation is strongly slowed and the lower value of polarization found for the nanoparticles ($P = 0.10$ and 0.40 for nanoparticles and dansylamide, respectively) shows that depolarization takes place by excitation energy migration in the dansyl network.¹¹ This mechanism of depolarization is anyway not completely efficient as proved by the residual anisotropy detectable even in solution ($P = 0.04$ in CHCl₃).

Protonation of Dansylated Nanoparticles 2. We investigated the photophysical properties of the nanoparticles and the effects of protonation both in a CH₃CN/CHCl₃ mixture (5/1 v/v) and in pure CHCl₃. Very diluted solutions ($c = 4.0 \times 10^{-9}$ M, corresponding to a concentration of the dansyl chromophore of 1.6×10^{-5} M) were used to avoid precipitation of the protonated species and to limit the spectral corrections.

The absorption spectrum of the particles presents the same typical absorption bands of dansyl derivatives described for the reference compound **1**.⁷ Also the fluorescence spectrum, the quantum yield, and the excited-state lifetime are very similar and show the same dependence on the polarity of the solvent (Tables 1 and 2).

In both the solvents, addition of CF₃SO₃H solutions causes in the absorption spectrum the gradual disappearance of the charge-transfer band around 340 nm and the growth of a new band at 287 nm as expected for the formation of Dns·H⁺. The

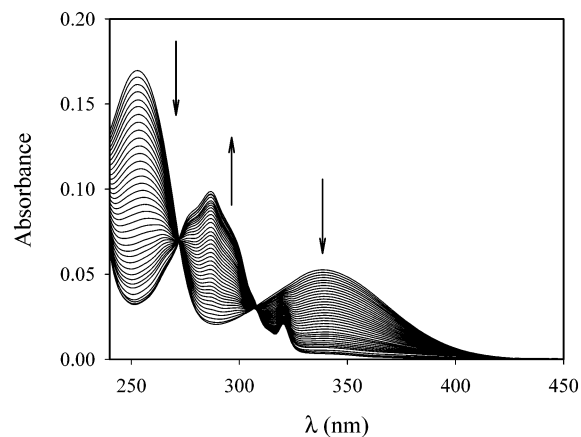


Figure 7. Absorption spectra of nanoparticles **2** ($c = 4 \times 10^{-9}$ M) in CH₃CN/CHCl₃ (5/1 v/v) upon addition of increasing amounts of CF₃SO₃H.

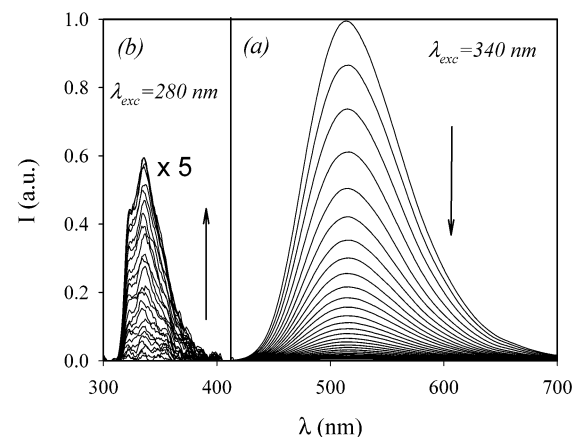


Figure 8. Fluorescence spectra of nanoparticles **2** ($c = 4 \times 10^{-9}$ M) in CH₃CN/CHCl₃ (5/1 v/v) during the titration with CF₃SO₃H.

absorption spectra recorded during the titration in CH₃CN/CHCl₃ are shown in Figure 7. The presence of two sharp isosbestic points at the same wavelengths as those found for **1** indicates that during the titration the absorption spectra are always the linear combination of the spectra of the appended chromophores Dns and Dns·H⁺, whose characteristics are unaffected by the constriction into the nanoscopic array.

This is extremely important since it allows us to evaluate the composition of the system, i.e., the fraction of protonated units, simply from the absorbance values. It is important to stress that, on the basis of the observations reported above, the absorption spectra of systems **1** and **2**, with the same composition, are almost identical, when solutions with the same concentration of dansyl units are used.

As far as luminescence is concerned, the protonation process causes a quenching of the dansyl fluorescence (Figure 8a, $\lambda_{exc} = 340$ nm) and the appearance of the typical naphthalene emission (Figure 8b, $\lambda_{exc} = 280$ nm). It is important to emphasize that also for nanoparticles **2** the corrected luminescence intensities of both Dns and Dns·H⁺ are not proportional to the respective concentrations calculated from the absorption spectra, indicating again the presence of intercomponent processes. In addition, the overall luminescence behavior is strongly affected by the nature of the solvent.

In Figure 9 it is possible to compare the different response to protonation of the Dns luminescence in **1** and **2** in the acetonitrile/chloroform solutions. The first interesting feature

(10) TEM pictures were elaborated with SigmaScan 5 and SigmaPlot 5 by SPSS Inc.

(11) Lakowicz, J. R. *Principles of Fluorescence Spectroscopy*; Kluwer Academic/Plenum Publishers: New York, 1999.

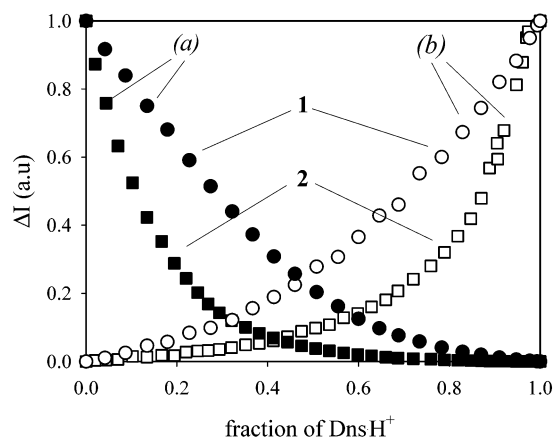


Figure 9. Normalized luminescence intensity changes of $\text{CH}_3\text{CN}/\text{CHCl}_3$ (5/1 v/v) solutions of **1** (8×10^{-6} M) and **2** (4×10^{-9} M) as a function of the degree of protonation calculated from the absorbance at 280 nm: (a) $\lambda_{\text{exc}} = 340$ nm, $\lambda_{\text{em}} = 510$ nm; (b) $\lambda_{\text{exc}} = 280$ nm, $\lambda_{\text{em}} = 340$ nm.⁹

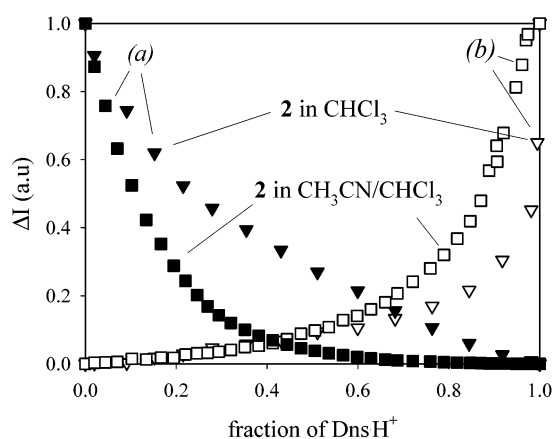


Figure 10. Normalized luminescence intensity changes of solutions of nanoparticles **2** ($c = 4 \times 10^{-9}$ M) in $\text{CH}_3\text{CN}/\text{CHCl}_3$ (5/1 v/v) and in pure CHCl_3 as a function of the degree of protonation calculated from the absorbance at 280 nm: (a) $\lambda_{\text{exc}} = 340$ nm, $\lambda_{\text{em}} = 510$ nm; (b) $\lambda_{\text{exc}} = 280$ nm, $\lambda_{\text{em}} = 340$ nm.⁹

is that, in the first part of the titration, the protonation of a single Dns unit in this solvent reduces the total luminescence to an extent comparable with the complete quenching of about five Dns units. It is worth recalling that for the reference compound **1**, under the same conditions, the ratio between quenched Dns moieties and $\text{Dns}\cdot\text{H}^+$ formed was close to 2. This different behavior is clearly depicted in Figure 9 by the different slopes of the decrease of Dns fluorescence for **1** and **2** on increasing the degree of protonation. Another interesting feature that can be evidenced from the same figure is that, as already observed for **1**, the luminescence of the $\text{Dns}\cdot\text{H}^+$ units formed in the first part of the titration is almost completely quenched, while it is switched on only when these units are in large excess. In other words, the switching on of the $\text{Dns}\cdot\text{H}^+$ luminescence is delayed with respect to the protonation, and this effect is much more evident in the nanoparticles than in the reference compound **1** (Figure 9).

In pure chloroform the situation is different, as can be qualitatively but clearly observed in Figure 10. The entity of the first effect observed, namely, the enhanced luminescence quenching of Dns fluorescence caused by protonation, is reduced, while the switching on of the $\text{Dns}\cdot\text{H}^+$ luminescence is further delayed, requiring the protonation of an even larger

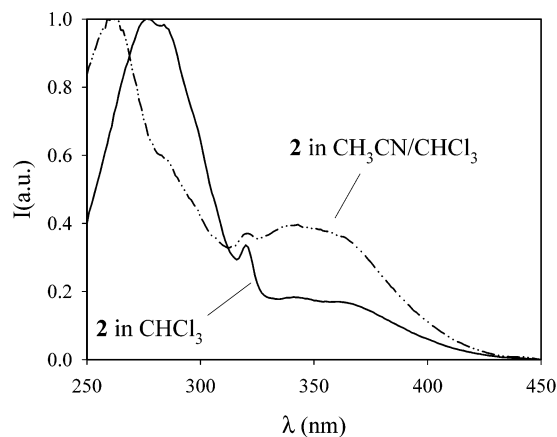


Figure 11. Excitation spectra of solutions of **2** ($c = 4 \times 10^{-8}$ M) in CHCl_3 and $\text{CH}_3\text{CN}/\text{CHCl}_3$ (5/1 v/v); $\lambda_{\text{em}} = 510$ nm after protonation of 90% of Dns units.

fraction of dansyl units with respect to what was observed in the acetonitrile/chloroform mixture.

The finding that protonation causes a more pronounced quenching in nanoparticles than in **1** can be easily explained by considering that when only a small fraction of dansyl units are protonated, each $\text{Dns}\cdot\text{H}^+$ moiety is surrounded by a large number of Dns fluorophores. As a consequence, in the nanoparticles the interactions responsible for the luminescence quenching can involve a large number of units. On the contrary, in the $\text{1}\cdot\text{H}^+$ species the $\text{Dns}\cdot\text{H}^+$ unit can interact only with the Dns of the same moiety, since in our experimental conditions bimolecular processes are unlikely to occur.

The delay in the switching on of the $\text{Dns}\cdot\text{H}^+$ luminescence can be explained in the same way. Also in this case a single Dns chromophore can interact with many $\text{Dns}\cdot\text{H}^+$ moieties and the protonation of a larger fraction of dansyl units is necessary to avoid quenching.

As was found for **1**, the quenching of the luminescence of the Dns unit can be again explained by the occurrence of a thermodynamically allowed charge-transfer process to a close-lying $\text{Dns}\cdot\text{H}^+$ unit. This explanation is in agreement with the noticeable dependence of the quenching efficiency on solvent polarity.

An even more interesting effect of the solvent on the fluorescence characteristics of the nanoparticles can be noticed by comparing the excitation spectra in acetonitrile/chloroform and in pure chloroform after protonation of 90% of the dansyl moieties. Although the absorption spectra are almost identical in the two solvents, the excitation spectra are very different. In particular, as can be seen from Figure 11, the contribution of the band associated with the absorption of the $\text{Dns}\cdot\text{H}^+$ species in the 240–315 nm region is much larger in the less polar solvent. Moreover, a direct comparison between the excitation spectra (Figures 5 and 11) indicates that in this latter solvent the energy transfer process already observed in the reference compound **1** is much more efficient in nanoparticles **2**. It is worth emphasizing that also the average luminescence quantum yield of the Dns moieties, toward which the excitation energy is conveyed, is higher in pure chloroform (Figure 12) because of a decrease in the rate of the electron-transfer process due to a lower stabilization of the intercomponent charge-separated state in the apolar solvent. Such a higher fluorescence efficiency is also confirmed by a larger contribution of longer excited-

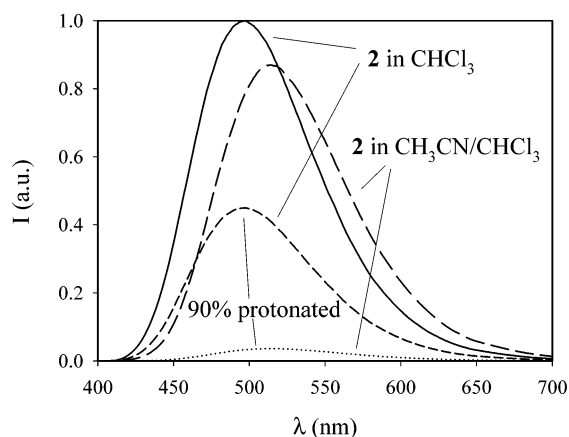


Figure 12. Fluorescence spectra of solutions of **2** ($c = 4 \cdot 10^{-8} \text{M}$) in CHCl_3 and $\text{CH}_3\text{CN}/\text{CHCl}_3$ 5/1, v/v; $\lambda_{\text{exc}} = 340 \text{ nm}$ before and after protonation of 90% Dns units.

state lifetime in the multiexponential decay of the dansyl luminescence signal.

These characteristics make nanoparticles **2** an antenna system whose efficiency can be strongly controlled on changing the nature of the solvent since, as has been shown, the polarity of the environment plays an important role in the delicate balance among different photophysical processes.

Conclusions

We have shown here that the reference bisdansylated compound **1** upon monoprotection shows an almost complete quenching of the typical fluorescence of both the Dns (a large band in the 440–600 nm region) and the $\text{Dns} \cdot \text{H}^+$ (a structured band in the 330–400 nm region) units. An energy transfer process from $\text{Dns} \cdot \text{H}^+$ to Dns was also observed, but with a quite low efficiency in both the solvents investigated.

Different behavior was instead shown by the dansylated nanoparticles **2**. In particular, they respond to protonation in a polar environment with an amplified quenching of the dansyl luminescence (up to five quenched units per added proton)^{2b} due to multicomponent charge-transfer processes. On the contrary, when protonated in pure chloroform they behave as an efficient antenna system, where the energy absorbed by the $\text{Dns} \cdot \text{H}^+$ is efficiently transferred to the luminescent Dns chromophore.^{2a} The different behavior observed in the two solvents can be conveniently explained by the role of environmental polarity on the delicate balance among different photophysical processes, such as fluorescence emission and energy- and electron-transfer processes.

On the other hand, the different behavior between **1** and **2** is due to the possible occurrence in an organized network, such as that present on the surface of nanoparticles, of photophysical processes involving a large number of chromophores, leading to large signal amplification even upon small chemical inputs. The tunability of the photophysical properties of these systems makes them extremely interesting for the design of new photoactive devices, especially in relation to the field of fluorescence-based sensors.^{1a}

Experimental Section

TEM Experiments. For TEM investigations a drop of nanoparticles solution in CH_2Cl_2 was transferred onto holey carbon foils supported on conventional copper microgrids. A Philips CM 100 transmission electron microscope operating at 80 kV was used.

Photophysical Experiments. Luminescence quantum yields were measured against a standard of quinine sulfate in 0.05 M H_2SO_4 ($\Phi = 0.564$) for the 400–600 nm region and naphthalene in cyclohexane ($\Phi = 0.23$) for the 300–400 nm region. The emission intensity was corrected for inner filter effects. Experimental details for the photophysical measurements are reported elsewhere.^{2a,12}

Preparation of 1,6-Bis(dansylamino)hexane (1). 1,6-Diaminohexane (1.0 mmol) was mixed with dansyl chloride (2.5 mmol) in the presence of tributylamine (2.5 mmol) as a base. All the reagents were purchased from Fluka. The reaction was carried out in boiling dichloromethane (10 mL) for 3 h under argon atmosphere. The product was purified by column chromatography (SiO_2 ; CH_2Cl_2).

After drying over $\text{Mg}(\text{SO}_4)_2$, vacuum evaporation yielded the pure product as a yellow fluorescent powder.

¹H NMR (200 MHz, CDCl_3 , δ (ppm)): 0.91 (m, 4H, $(\text{NCH}_2\text{CH}_2\text{CH}_2)_2$), 1.24 (m, 4H, $(\text{NCH}_2\text{CH}_2\text{CH}_2)_2$), 2.77 (m, 4H, $(\text{NCH}_2\text{CH}_2\text{CH}_2)_2$), 2.90 (s, 6H, $\text{N}(\text{CH}_3)_2$), 7.12 (d, 2H, CH_{Dns}), 7.52 (m, 4H, CH_{Dns}), 8.25 (m, 4H, CH_{Dns}), 8.52 (d, 2H, CH_{Dns}); ESI-MS m/z 583.3 [$\text{M} + \text{H}^+$].

Preparation of (3-Dansylaminopropyl)trimethoxysilane (3). (3-Aminopropyl)trimethoxysilane (1.0 mmol) was added to 1.5 mmol of dansyl chloride and stirred for 2 h in boiling CH_2Cl_2 in the presence of tributylamine (1.5 mmol). All the reagents were purchased from Fluka. The complete substitution of the amino group was evidenced by TLC (SiO_2 ; CH_3CN) and ¹H NMR. Dichloromethane was removed by vacuum evaporation and a yellow, strongly fluorescent oil was obtained. The crude product was purified by column chromatography (SiO_2 ; CH_2Cl_2) to yield **3**.

¹H NMR (200 MHz, CDCl_3 , δ (ppm)) 0.56 (m, 2H, $\text{NCH}_2\text{CH}_2\text{CH}_2\text{Si}$), 1.46 (m, 2H, $\text{NCH}_2\text{CH}_2\text{CH}_2\text{Si}$), 2.94 (m, 8H, $\text{NCH}_2\text{CH}_2\text{CH}_2\text{Si}$ and $\text{N}(\text{CH}_3)_2$), 3.56 (s, 9H, $\text{NCH}_2\text{CH}_2\text{CH}_2\text{Si}(\text{OCH}_3)_3$), 7.10 (d, 1H, CH_{Dns}), 7.54 (m, 2H, CH_{Dns}), 8.24 (t, 2H, CH_{Dns}), 8.54 (d, 1H, CH_{Dns}); ESI-MS m/z 413.0 [$\text{M} + \text{H}^+$].

Preparation of Dansylated Silica Nanoparticles (2). The product obtained from the previous reaction was dissolved in 5 mL of ethanol. Water (5 mL), 5 mL of CH_3COOH , and 500 μL of silica nanoparticles solution (30% w/w AS-30 from Aldrich) were added, and the mixture was refluxed at 80 °C for 2 days.

Ethanol was removed by evaporation under reduced pressure and nanoparticles were precipitated by increasing the pH to 6.0 by addition of solid NaHCO_3 . The resulting strongly luminescent yellow solid was filtered and washed five times with a borate buffer solution (pH 9.5) and five times with pure water.

The product was then dissolved in dichloromethane, and nanoparticles were precipitated by acidification with $\text{CF}_3\text{SO}_3\text{H}$. In these conditions all the products coming from the hydrolysis of the excess of **3** were removed by filtration.

The precipitated was washed 5 times with pure dichloromethane, dried, and dispersed in pure water. The purified nanoparticles were then extracted with dichloromethane by adding 1 mL of ammonia solution (37% w/w). The organic phase was isolated, and after drying over $\text{Mg}(\text{SO}_4)_2$ and solvent removal, a yellow highly fluorescent powder was obtained. Further purification by gel-permeation chromatography was carried out.

¹H NMR (200 MHz, CDCl_3 , δ (ppm)) 0.25 (2H, $\text{NCH}_2\text{CH}_2\text{CH}_2\text{Si}$), 1.28 (2H, $\text{NCH}_2\text{CH}_2\text{CH}_2\text{Si}$), 2.62 (2H, $\text{NCH}_2\text{CH}_2\text{CH}_2\text{Si}$), 2.66 (6H, $\text{N}(\text{CH}_3)_2$), 7.06 (1H, CH_{Dns}), 7.54 (2H, CH_{Dns}), 8.02 (2H, CH_{Dns}), 8.18 (1H, CH_{Dns}).

Acknowledgment. We thank Dr. Paola Ceroni for her help in the electrochemical measurements and MURST (Solid Supermolecules Project) and the University of Bologna (funds for selected topics) for the financial support.

JA027270X

(12) Charbonniere, L. J.; Ziessel, R.; Montalti, M.; Prodi, L.; Zaccheroni, N.; Boehme, C.; Wipff, G. *J. Am. Chem. Soc.* **2002**, *124*, 7779.